© 2014 IJIRT | Volume 1 Issue 6 | ISSN : 2349-6002

Enhance Patch-Antenna Performance through implementing Photonic-Bandgap Substrates

Dharmender Aswal, Krishna Sharda, Mahipal Butola

Student (B.Tech 5th sem) Department of Electronics and Comm. Engineering

Dronacharya Colege of Engineering, Gurgaon, Haryana

ABSTRACT: **The microstrip patch antenna is a low-profile robust planar structure. A wide range of radiation patterns can be achieved with this type of antenna and, due to the ease of manufacture, is inexpensive compared with other types of antennas. However, patch-antenna designs have some limitations such as restricted bandwidth of operation, low gain, and a potential decrease in radiation efficiency due to surface-wave losses. In this paper, a photonic-bandgap (PBG) substrate for patch antennas is proposed, which minimizes the surface-wave effects. In order to verify the performance of this kind of substrate, a configuration with a thick substrate is analyzed. The PBG patch antenna shows significantly reduced levels of surface modes compared to conventional patch antennas, thus improving the gain and far-field radiation pattern.**

I.INTRODUCTION

This century has seen substantial advances in semicon-ductor physics, which have allowed us to tailor the conducting properties of certain materials thereby initiating the transistor revolution in electronics. Within the last decade, there has been a breakthrough in the control of the optical properties of materials allowing us to control the emission and propagation of light [1]. Many major discoveries in physics in this century originate from the study of waves in periodic structures, examples include X-ray and electron diffraction by crystals, electronic band structure and holography. Photonic-bandgap (PBG) materials are a new class of periodic dielectrics, which are the photonic analogs of semiconductors. Electromagnetic waves behave in photonic crystals (PC's) as electrons behave in semiconductors [2]. These artificially engineered periodic materials, which control the propagation of electromagnetic waves, may play a role that is as important in the field of photonics as the laser playstoday in optoelectronic systems.

A periodic structure is characterized by two parameters: a spatial period defining the lattice constant and the dielectric contrast between the constituent materials. PBG crystals have a further property of gap dimensionality, which is directly related to the number of dimensions of the structure that are periodic. Within these periodic structures, the electromagnetic-mode distributions and their dispersion relations differ signif-

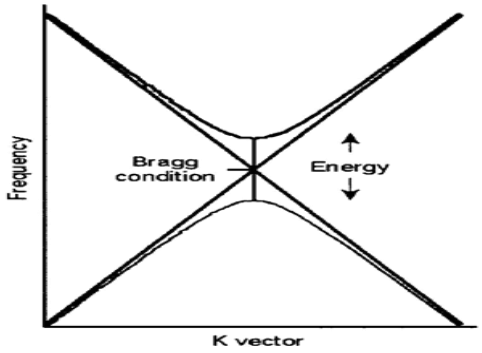

Fig. 1. Plot showing an example of the dispersion relation and the Bragg condition.

icantly from those of free space. Although one-dimensional PC's have been around for decades in the form of highly reflecting dielectric coatings for mirrors, (also known as Bragg stacks), the idea of making a two- or three-dimensional pho-tonic crystal is only about ten years old.

Within a one-dimensional periodic structure, the electromagnetic dispersion relation has frequency regions in which propagating electromagnetic modes are forbidden. In such forbidden frequency gaps or ªBragg frequencies,º electromagnetic waves attempting to propagate experience exponential attenuation due to Bragg reflections (Fig. 1). Although it has been shown that omnidirectional reflection can be achieved with a one-dimensional periodicity, this is only true when the point source of waves is not placed close to the crystal structure [3], [4]. By extending the periodicity from one to three dimensions [5], [6], it is possible to control the electromagnetic propagation for the entire three-dimensional space. A structure that is periodic in only one dimension will have a one-dimensional PBG, while another correctly designed structure that is periodic in all three dimensions can

display a fully three-dimensional PBG. The resultant relations. Such discontinuous regions are called ªpseudogapsº [7]. Within a pseudogap, propagating waves can have energies or frequencies only at certain -points, their existence at the other -points being forbidden. When the forbidden region extends to cover all propagation directions in the dispersion relation, the resultant gap is then particularly defined as a ªbandgap.º A PC prohibits photon propagation irrespective of the propagation direction.

Since their discovery, interest in PC's has grown explo-sively. The promise of applications using PC's such as highly efficient microwave devices and optical lasers, by significantly improving their efficiency, has spurred the excitement of this new multidisciplinary field of study. Another exciting appli-cation for PC's is as a substrate for antenna configurations.

An antenna that is placed on a high-permittivity dielectric substrate may couple power into substrate modes. As substrate modes do not contribute to the primary radiation pattern, these modes are a loss mechanism. PC's can offer a real solution to this problem. Utilized in patch-antenna configurations as substrates, PC's suppress both substrate modes and surface waves that would otherwise be excited in the substrate by the radiating element. Suppression or reduction of surface waves improves antenna efficiency and reduces the sidelobe level that is caused by the diffraction of surface waves at the edges of the antenna substrate [8]±[12]. Surface-wave diffraction plays a major role when thick substrates are used to increase the bandwidth of the antenna. Power losses due to surface waves can be as high as 60% of the radiated power when thick substrates with high dielectric constant value are used.

In Section II, a brief description explaining the fundamental parameters that define crystal structures will be presented. Section III will present the electromagnetic theory used to analyze periodic crystal structures. Section IV examines the patch-antenna design, Section V considers the specific PC structure, a square lattice of air columns, which will be used as substrate in the patch-antenna configuration. Finally, Section VI presents and discusses the results obtained for the patch antenna on a PBG substrate.

II. CRYSTAL STRUCTURES

Ideal PC's are made from an infinite number of tiled arbitrarily identically shaped ªatomsº (to stress the analogy with semiconductors), which repeat to form either a one-, two-, or three-dimensional periodic lattice [10]. Some examples of unit cells of PC's are illustrated in Fig. 2. Each PC can generate a characteristic PBG because of interactions between multiple scattering from the lattice and from scattering by individual atoms. PC's are generally characterized by the following independent variables:

1) lattice structure (lattice constant);

2) shape of the individual atoms;

3) fill factorÐratio between volume of atoms in the unit cell and volume of the unit cell;

4)dielectric constants of the constituent materials.

A specific combination of these variables can lead to a desirable PBG in dispersion relation. In this section, a brief summary covering the basic lattice parameters such as the

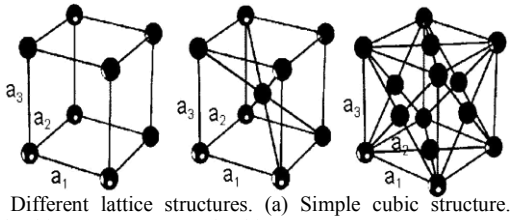

Fig. 2. Different lattice structures. (a) Simple cubic structure. (b) Body centered cubic. (c) Face centered cubic.

primitive lattice, reciprocal lattice, and the Brillouin zone is presented, which define a crystalline structure, following the notation presented in [13].

A. Primitive Lattice

The structure of all crystals can be described in terms of lattice vectors, with a group of atoms attached to every lattice point called the ªbasisº of the lattice. The basis is repeated in space to form the crystalline structure. The basis consists of a primitive cell, arranging one cell at each lattice point will fill up the entire crystal without leaving undefined voids or overlapping regions. The Bravais lattice vectors describe how these repeating units in a crystal are tiled. A Bravais lattice can be defined as all points with positions

$$\vec{R} = n_1\vec{a}_1 + n_2\vec{a}_2 + n_3\vec{a}_3 \quad (1)$$

where $\vec{a}_i$ are not in the same plane, and n_i are integers. The $\vec{a}_i$ vectors are called the primitive vectors and there are many possible choices of these vectors. The Wigner±Seitz [13] cell is the most common choice for the primitive unit cell. This defines a region of space that is closer to a particular point

rather than to any other point on a Bravais lattice.

B. Reciprocal Lattice

The reciprocal lattice is a Bravais lattice itself, but it is defined in k space. The reciprocal lattice can be defined as all k that satisfy

$$k = m_1 b_1 + m_2 b_2 + m_3 b_3 \tag{2}$$

where m_i are integers and $\vec{b}_i$ are the reciprocal vectors. The $\vec{b}_i$ vectors are generated by satisfying the following relation:

$$\begin{aligned}\vec{k} \cdot \vec{R} &= (n_1 \cdot \vec{a}_1 + n_2 \cdot \vec{a}_2 + n_3 \cdot \vec{a}_3) \cdot (m_1 \cdot \vec{b}_1 + m_2 \cdot \vec{b}_2 + m_3 \cdot \vec{b}_3) \\ &= N \cdot 2 \cdot \pi \end{aligned} \tag{3}$$

For all choices of n_i and m_i, the above condition must hold for some N. This condition is satisfied if the b_i are chosen such that $\vec{a}_i \cdot b_j = 2\pi\delta_{ij}$. In this way, the following primitive reciprocal lattice vectors are obtained:

$$b_1 = 2 \cdot \pi \frac{\vec{a}_2 \times \vec{a}_3}{\vec{a}_1 \cdot (\vec{a}_2 \times \vec{a}_3)} \tag{4}$$

$$\rightarrow \qquad \vec{a}_3 \times \vec{a}_1$$

$$b_2 = 2 \cdot \pi \frac{\vec{a}_1 \times \vec{a}_2}{\vec{a}_1 \cdot (\vec{a}_2 \times \vec{a}_3)} \tag{5}$$

$$\vec{b}_3 = 2 \cdot \pi \frac{\vec{a}_1 \times \vec{a}_2}{\vec{a}_1 \cdot (\vec{a}_2 \times \vec{a}_3)}. \tag{6}$$

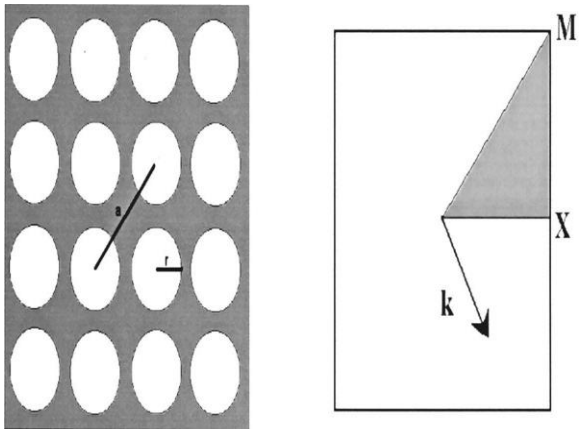

Fig. 3. PC made using a square lattice. (Right-hand side: Brillouin zone of this square lattice). The irreducible zone is depicted in the dark shading.

In summary, when the Fourier transform of a function that is periodic on a lattice is required, it is only necessary to include terms with wave vectors that are reciprocal lattice vectors. The Wigner±Seitz cell of the reciprocal lattice is called the first Brillouin zone.

C. The Brillouin Zone

The study of waves in periodic structures makes use of a single physical principle proposed by Floquet in 1884. The principle states that normal modes in periodic structures can be expressed as a superposition of a set of plane waves whose wave vectors are related by: $k_n = k_0 + nG$, where k_0 is the initial arbitrary wave vector, k_n is the wave vector of the nth mode, and G is the reciprocal lattice vector. Later extension of the theorem by Bloch covered multidimensional periodic structures in his treatment of electrons in a crystal and is referred to as the Bloch expansion. The modes can be written in Bloch form as

$$H_k(r) = e^{ik_r} u_k(r) = e^{ik_r} u_k(r + R). \tag{7}$$

Bloch states have a fundamentally important feature; dif-

ferent values of k do not necessarily lead to different modes. Specifically, a mode with wave vector $\vec{k}$ and a mode with wave vector $(\vec{k} + \vec{G})$ are the same mode if $\vec{G}$ is a reciprocal

lattice vector.

Consequently, there is redundancy in the label k and we can restrict our attention to a finite zone in reciprocal space. Within this zone, it is not possible to translate from one part of the volume to another through the addition any reciprocal lattice vector G. Values of k that lie outside of this zone can be reached from within the zone by adding G and are, therefore, redundant labels. This zone is the Brillouin zone.

The smallest region within the Brillouin zone for which the k directions are not related by symmetry is called the *irreducible* Brillouin zone. For example, a PC with the symmetry of a simple square lattice has a square Brillouin zone centered at $k=0$, as depicted in Fig. 3. The *irreducible* zone is a triangular wedge with 1/8 the area of the full Brillouin zone defined by the Γ, X, M points; the rest of the Brillouin zone contains redundant copies of the irreducible zone.

III. ELECTROMAGNETIC FIELDS IN PC'S

There is active investigation into efficient theoretical methods to evaluate dispersion relations in PC's and many theoretical methods have been proposed based on numerical computations. The plane-wave method, a powerful and suc-

cessful method in the photonic band theory, generates various kinds of eigensystems readily compatible with commercial or public eigensystem solution package routines. The matrix equations and eigensystems formulated here are entirely based in Cartesian coordinates and are readily extendible to describe more general PC's with conductive, absorptive, or active media.

Macroscopic electromagnetism, including the propagation of light in a PC, is governed by the four Maxwell equations. In the medium in which the equation will be solved, we assume that the material is macroscopic and isotropic, thus, $\vec{D}$ and $\vec{E}$ are related by a scalar dielectric constant $\varepsilon(r,\omega)$. With this definition, it is important to note that the $E(r,\omega)$ $D(r,\omega)$ dependence of the dielectric constant with position has been established. While a PC structure, such as a substrate with holes, could be thought of as a nonisotropic medium, the anisotropy is introduced into the equations through positional dependence of the dielectric constant. Frequency dependence of the dielectric constant will be ignored, and $\varepsilon(r)$ will be taken as real, indicating an ideal dielectric.

Using the ratio $\vec{D}(r) = \varepsilon(r)\vec{E}(r)$ and taking into account that the relative magnetic permeability is very close to unity, the Maxwell's equations can be written as

$$\nabla \cdot \vec{H}(r,t) = 0 \tag{8}$$

$$\nabla \cdot \varepsilon(r) \cdot \vec{E}(r,t) = 0 \tag{9}$$

$$\nabla \times \vec{E}(r,t) = -\frac{\partial}{\partial t}\vec{B}(r,t) \tag{10}$$

$$\nabla \times \vec{H}(r,t) = \frac{\partial}{\partial t}\varepsilon(r) \cdot \vec{E}(r,t) \tag{11}$$

The equations have been restricted to linear and lossless material. PC's made from nonlinear dielectrics are certainly of great interest and deserve a separate investigation, but are not covered in this paper. These equations can then be used to formulate the equation system for eigenvalues and eigenvectors in a PC.

Since the relative electric permittivity is a periodic function of position, the magnetic field satisfies Bloch's theorem and will also be divergence-free $(\nabla \cdot \vec{H} = 0)$ this is important in defining the *transverse* condition, which requires that if $H(r) = a \cdot \exp(ik \cdot r)$ then $a \cdot k = 0$ Satisfying these requirements allows the magnetic field to be expanded in a plane-wave basis as follows:

$$\begin{aligned} H(r,t) &= \sum_n \int_\Omega dk \cdot H_{n,k}(r,t) \\ &= \sum_n \int_\Omega dk \cdot f_{n,k} \sum_G \sum_{l=1}^{2} h_{n,k}(k+G) \cdot \hat{e}_l(k+G) \\ &\quad \cdot \exp\left[i(k+G) \cdot r - i\omega_{n,k}t\right] \qquad (12) \qquad (12) \end{aligned}$$

where n is the band index, k is the wave vector in the first Brillouin zone, G is the reciprocal lattice vector, $\omega_{n,k}$ is the angular frequency corresponding to the given wave vector, l is the polarization index, and $\hat{e}_1(k+G)$ and $\hat{e}_2(k+G)$ are polarization unit vectors such that $\{\hat{e}_1(k+G), \hat{e}_2(k+G), (k+G)/|k+G|\}$ form a right-handed triad. The factor $f_{n,k}$ is an expansion coefficient of an arbitrary magnetic field in terms of eigensolutions.

Following the description given in [14], the final system obtained for the magnetic field is

$$\begin{aligned} &\sum_{G'} |k+G||k+G'|\eta_{G-G'} \\ &\quad \times \begin{bmatrix} \hat{e}_2(k+G)\cdot\hat{e}_2(k+G') & -\hat{e}_2(k+G)\cdot\hat{e}_1(k+G') \\ -\hat{e}_1(k+G)\cdot\hat{e}_2(k+G') & -\hat{e}_1(k+G)\cdot\hat{e}_1(k+G') \end{bmatrix} \\ &\quad \times \begin{pmatrix} h_{n,1}(k+G') \\ h_{n,2}(k+G') \end{pmatrix} \\ &\quad = \frac{\omega_{n,k}^2}{c^2} \begin{pmatrix} h_{n,1}(k+G) \\ h_{n,2}(k+G) \end{pmatrix}. \end{aligned} \tag{13}$$

This result leads to a standard matrix diagonalization problem for the eigenvectors and eigenvalues. Upon solution of (13), the dispersion relation for the PC is obtained.

Using the equation $E(r) = (\frac{}{\omega\varepsilon(r)})\nabla \times H(r)$, the electric field can be obtained.

It should be pointed out that this analysis assumes an infinitely periodic structure

IV. PATCH-ANTENNA DESIGN

This section describes the patch-antenna configuration that is selected to perform the comparison between using a normal substrate and a PBG substrate. The patch antenna is rectangular with 52-mm width and 25.96-mm length. The substrate has a dielectric constant of ten and a size of 420 mm × 420 mm × 10 mm. The antenna is placed in the middle of this substrate, as

shown in Fig. 4. The transmission line, designed to feed the patch antenna, is formed by a 50-Ω line together a quarter-wavelength transformer for impedance matching.

The size of the substrate is relatively large compared to the patch-antenna size. This has been done to allow comparison

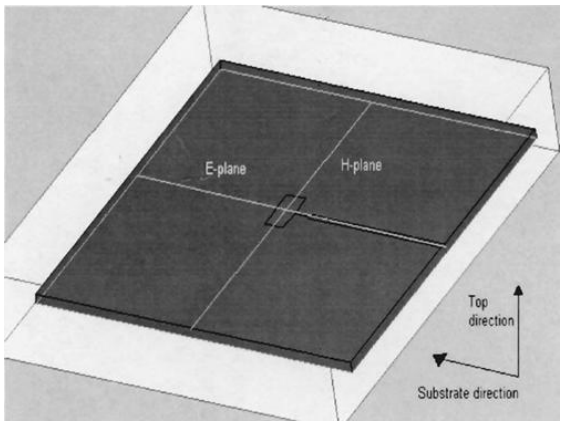

Fig. 4. The conventional patch antenna on a substrate with a dielectric constant of ten.

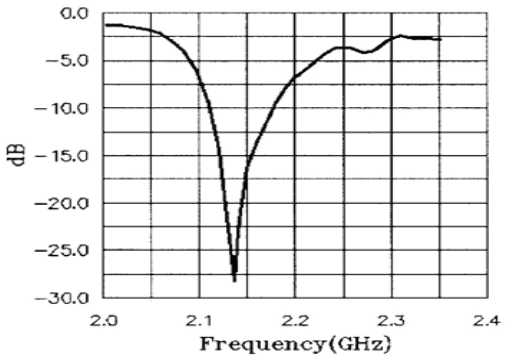

Fig. 5. Return loss ( ) for the conventional patch antenna.

Section VI). Furthermore, a comparison between the generation of surface mode in both configurations will be performed. To analyze the performance of the antenna, the commercial finite-element software package HP-HFSS was used. Fig. 5 shows the calculated return loss (S_{11}) of the patch antenna. The point of resonance corresponds to 2.14 GHz, so this will be the working frequency. The far-field radiation patterns obtained at 2.14 GHz are shown in Fig. 6. The maximum directivity is 6.7 dB. It can be observed that the different cuts present a lot of ripple due to the addition of the fields from the surface waves originating at the edges of the substrate with the direct pattern from the patch antenna. In this case, this effect can probably be attributed to the TM_0 surface mode since this mode has no cutoff. As a rule of thumb, surface-mode excitation becomes appreciable when $h/\lambda_0 > 0.03$ for $\varepsilon_r \approx 10$ [15]; for this case, the value is 0.07, indicating that surface-wave contributions will not be negligible.

The definition of surface waves used is equivalent to the one for modes that propagate along a dielectric sheetÐthese are often called ªtrappedº modes [16].

Using the equation $f_c = nc/(4 \cdot h \cdot \sqrt{\varepsilon - 1})$ where h is the substrate thickness, ε is the substrate dielectric constant, and with $n = 1$, the cutoff frequency for the first TE_1

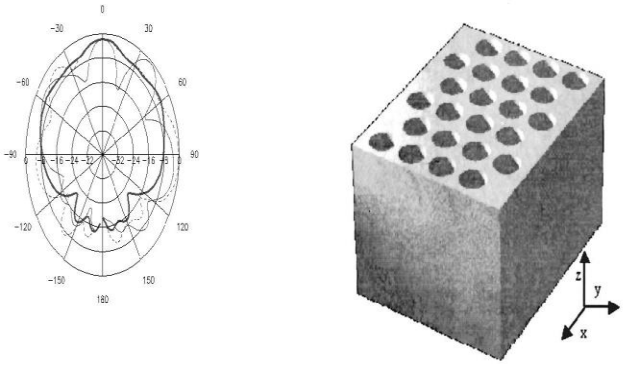

Fig. 6. Far-field radiation pattern from the conventional patch antenna. Each division corresponds to 10 dB. The blue line signifies the H-plane cut and the green line signifies the E-plane. The red and pink lines are the 45 and 135 cuts.

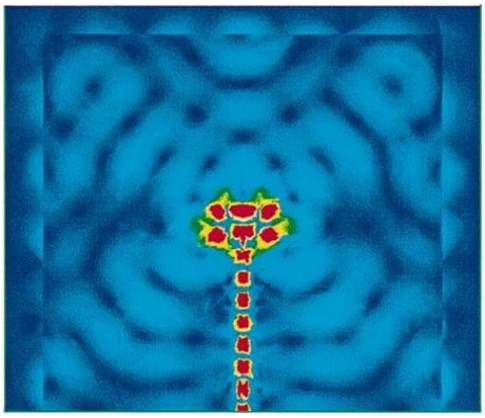

Fig. 7. Surface plot of the electric field of the patch-antenna configuration. Red signifies maximum power while dark blue signifies minimum power.

surface mode is 2.5 GHz. This value is safely away from the working frequency, thus, the assumption that only the TM_0 mode is propagating is justified. Further demonstration of the

existence of the substrate mode is given in Fig. 7, which shows the magnitude of the electric field in a transverse cut of the patch antenna at the frequency of operation of 2.14 GHz. The existence of the substrate mode is clearly visible.

V. PBG DESIGN

While the previous section has defined the patch-antenna configuration for which the effect of surface mode generation has to be minimized, we now present the design of the PBG substrate. Different kinds of PBG structures can be used as substrates, but for simplicity, the proposed structure is a square lattice of air columns embedded in a dielectric medium (see Fig. 8) [17]±[19]. The dielectric material is again taken as having a dielectric constant $\varepsilon_r = 10$.

Before embarking upon the electromagnetic study of this PC structure, the primitive lattice vectors, the reciprocal lattice vectors, and the Brillouin zone will be defined. The direct lattice of a two-dimensional structure, periodic in the x±y- plane, is described by two main vectors placed in the same periodic plane. As the two-dimensional PC is formed by a square lattice, the vectors that define the direct lattice for this lattice can be written as

$$\begin{aligned} \hat{a}_1 &= a \cdot \hat{x} \\ \hat{a}_2 &= a \cdot \hat{y} \end{aligned} \tag{14}$$

where a is any lattice size, thus, the structure is defined in normalized units. Another parameter that will be used to define the structure is the r/a ratio, where r is the radius of the column. With the primitive lattice vectors defined, the reciprocal lattice vectors can now be fixed. Using (3), the vectors are defined as

$$\begin{aligned} \hat{b}_1 &= \frac{2 \cdot \pi}{a} \hat{y} \\ \hat{b}_2 &= \frac{2 \cdot \pi}{a} \hat{x} \end{aligned} . \tag{15}$$

The irreducible Brillouin zone is the triangular wedge in the upper right-hand-side corner of Fig. 3; the rest of the Brillouin zone can be related to this wedge by rotational symmetry. There are three special points: Γ, X, and M, which are corresponded, respectively, to $k = 0 k = (\pi/a)\hat{x} k = (\pi/a)\hat{x} + (\pi/a)\hat{y}$, which completely describe the irreducible Brillouin zone that is also shown in Fig. 3. Sweeping over this zone, all directions in the k-space of the propagating incident waves will have been taken into account, fully characterizing the dispersion relation for the PC.

After defining the PBG structure, the dispersion relation for this structure was calculated. The so-called "gap map" [1] for the structure is obtained by fixing the dielectric constant and sweeping the *r/a* ratio. The gap map then allows us to choose the *r/a* value to maximize the available PBG for the desi frequency of operation. Fig. 9(a) and (b) shows the TE and TM polarization gap maps, respectively, with a dielectric constant of ten. Along the horizontal axis of the gap map is the r/a ratio of the columns and along the vertical axis is the normalized frequency $(f.a/c)$.

Using these maps and taking a working frequency of 2.14 GHz, the lattice size (a) can be obtained. There are

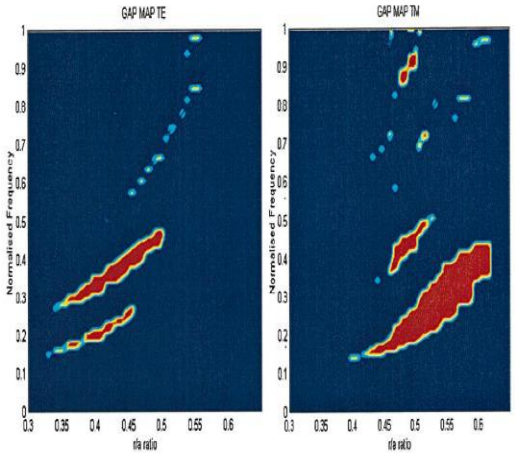

Fig. 9. (a) Gap map for TE and (b) TM polarizations in the case of air columns in a dielectric substrate with "r = 10.

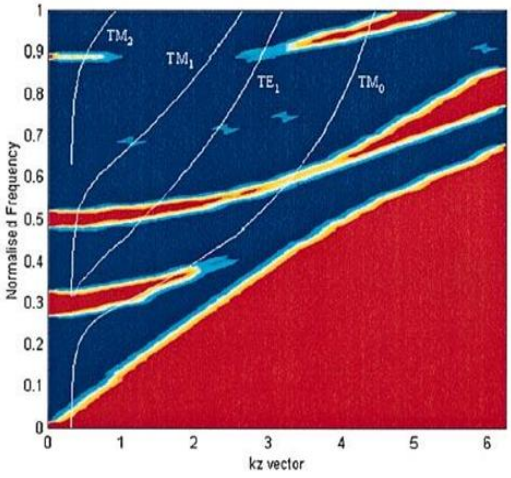

Fig. 10. Dispersion diagram for TM polarization of the PBG configuration under study as a function of kz together with the dispersion diagram for the surface-wave modes of the

dielectric sheet.

different possibilities, but the selection criteria will be governed by minimizing the total device size. It was already stated that the only surface mode in propagation is the TM_0, thus, one only has to consider the TM polarization map. With these two premises, the selected r/a value was 0.48 together with a normalized frequency 0.27, giving a lattice period of 38 mm.

It is clear that the TM_0 surface mode in the host material has a discrete normalized k_z component for each frequency. The previous gap maps were obtained assuming that the propagation was in the $X \pm Y$ -plane with $k_z = 0$. However, out-of-plane propagation of electromagnetic waves must be taken into account as k_z is nonzero [1], [20]. Fig. 10 shows the gap map for TM polarization of the PBG structure with $r/a = 0.48$ and a dielectric constant of ten as a function of

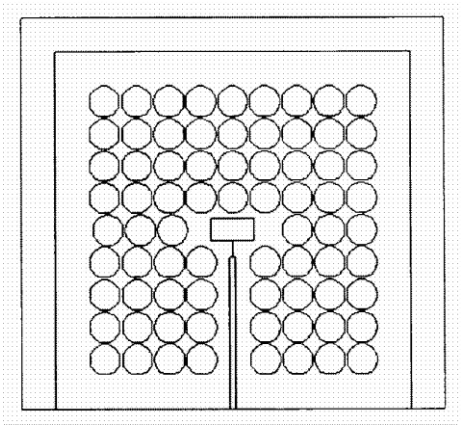

Fig. 11. Patch antenna on a PBG substrate formed by four holes in a square lattice with dielectric constant of ten.

Superimposed to this figure, the discrete curves for TM_n and TE_n surface-wave modes in the dielectric slab are plotted. It is observed that for the normalized working frequency 0.27, the TM_0 surface-wave mode is again the only mode in propagation. It should also be clear that the limitation in upper frequency will be determined by the cutoff frequency of the TE_1 surface-wave mode because this specific PBG structure is not designed to suppress TE polarized surface modes.

VI. PATCH ANTENNA ON A PBG SUBSTRATE

Now that the PBG structure that will be used as substrate of the patch antenna has been defined, the properties of this configuration will be studied. The configuration dimensions were defined in Section IV and the software used to simulate the behavior of this structure was HP-HFSS. Convergence and minimization of errors were obtained by ensuring that enough iterations were used.

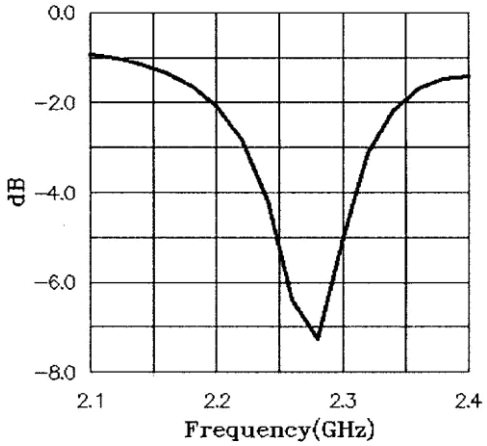

Fig. 12. Input return loss ( ) for the antenna patch on a PBG substrate.

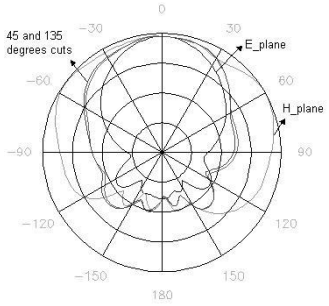

Fig. 13. Far-field radiation pattern from the patch antenna on a PBG substrate. Each division corresponds to 10 dB.

Fig. 11 shows the structure under study, where four columns of holes have been added in order to suppress the surface mode. The calculated input return loss for this design is shown in Fig. 12. The resonance frequency has shifted to 2.27 GHz due to the variation in the effective dielectric constant, and S_{11} at this frequency has degraded with respect to that of the patch antenna without PBG. A possible reason for this is the fact that the holes are reflecting the surface mode, returning the power across the feed line. Different designs are under development in order to improve the input return loss for this kind of structures.

The far-field radiation patterns obtained at 2.27 GHz are shown in Fig. 13. The maximum directivity is 8.8 dB. It can be observed that the different cuts do not present a ripple. This is indicating that the surface mode has been reduced

considerably. In order to verify this claim, Fig. 14 shows the surface plot of the electric-field magnitude, which can be compared with Fig. 7. Both plots have been normalized at the same maximum and minimum values.

Looking at the $_E$ plane cut in the radiation pattern Fig.13, it can be clearly seen that the patterns broa
and that there are two peaks. These peaks are due to the radiation from the feed line, which probably can be avoided by improving the feeding technique.

It should be noted that for 2.23 GHz, the S_{11} for both designs has the same value. Therefore, this frequency point has been selected to perform an additional comparison between the two designs. The radiation patterns for the conventional patch

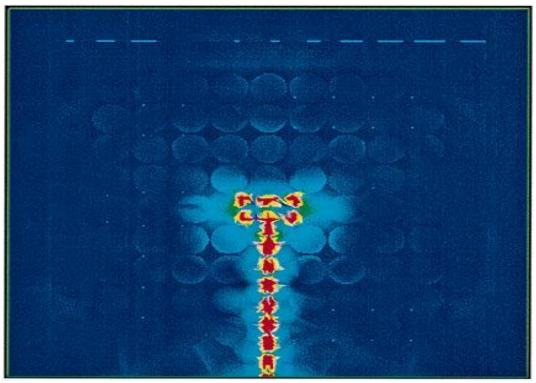

Fig. 14. Surface plot of the electric field in the PBG patch-antenna config-uration. Red signifies maximum power while dark blue signifies minimum power.

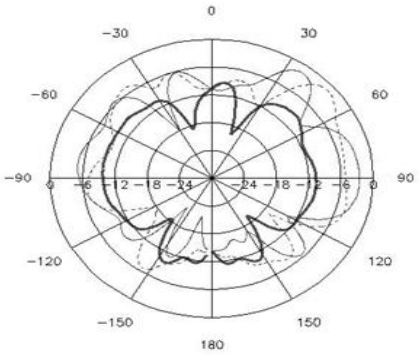

Fig. 15. Far-field radiation pattern at 2.23 GHz from the normal patch. Each division corresponds to 10 dB. The maximum directivity is 8.15 dB. The thick solid line is the H-plane cut, the thin solid line is the E-plane, and the dashed line is the 45 cut.

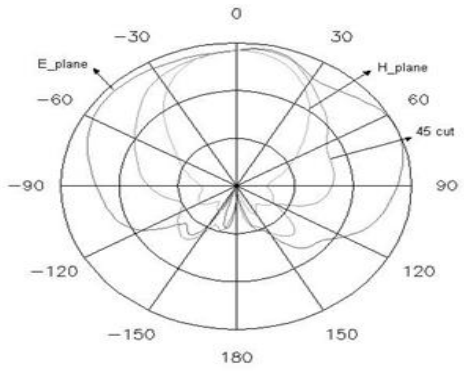

Fig. 16. Far-field radiation pattern at 2.23 GHz from the PBG patch. Each division corresponds to 10 dB. The maximum directivity is 9 dB.

antenna and PBG antenna at 2.23 GHz are shown in Figs. 15 and 16, respectively. The gain in the forward direction for the conventional case is 2 dB and in the PBG case is 7.75 dB. This means that an improvement in the gain of approximately 10 dB has been obtained.

VII. CONCLUSION

Comparisons between the results from a conventional patch antenna to a patch antenna on a PBG substrate show that the reduction in the surface mode level is remarkable. This can be observed in the radiation pattern (the ripple due to surface modes has almost disappeared) and in the surface plots (the levels have been reduced). This will lead, of course, to anincrease in the antenna efficiency.

The back radiation is also considerably reduced. In the case of a conventional patch antenna working at 2.14 GHz, this ratio is 17 dB and, for 2.23 GHz, is around 12 dB. The PBG antenna presents a forward back ratio of 24 dB, indicating, in general, a lower back-plane radiation.

Due to the feeding technique used, the expected improvements in the bandwidth cannot be analyzed. Future designs will try to overcome this problem and allow to investigate the bandwidth performance. The shift in the resonance frequency will also be studied.

It is clear that PBG's offer promising potential applications in array configurations, increasing the antenna efficiency together with the suppression of its mutual coupling through the substrate material.

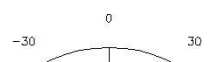

REFERENCES

[1] J. D. Joannopoulus, R. Meade, and J. Winn, *Photonic Crystals. Molding the Flow of Light*. Princeton, NJ: Pinceton Univ. Press, 1995.

[2] E. Yablonovitch, ªPhotonic crystals,º *J. Modern Opt.*, vol. 41, no. 2, pp. 173±194, 1994.

[3] J. N. Winn, Y. Fink, S. Fan, and J. D. Joannopoulos, ªOmnidirectional reflection from a one-dimensional photonic crystal,º *Opt. Lett.*, vol. 23, no. 20, pp. 1573±1575, Oct. 15, 1998.

[4] E. Yablonovitch, ªEngineered omnidirectional external-reflectivity spec-tra from one-dimensional layered interference filters,º *Opt. Lett.*, vol. 23, no. 21, pp. 1648±1649, Nov. 1998.

[5] E. Ozbay *et al.*, ªMeasurements of a three-dimensional photonic bandgap in a crystal structure made of dielectric rods,º *Phys. Rev. B, Condens. Matter*, vol. 50, no. 3, July 15, 1994.

[6] H. S. Souzer and J. P. Dowiling, ªPhotonic band calculation for woodpile structures,º *J. Modern Opt.*, vol. 41, no. 2, pp. 231±339, 1994.

[7] P. Russel, ªPhotonic bandgaps,º *Phys. World*, pp. 37±42, Aug. 1992.

[8] E. R. Brown, C. D. Parker, and E. Yablonovitch, ªRadiation properties of a planar antenna on a photonic-crystal substrate,º *Opt. Soc. Amer. B*, vol. 10, no. 2, Feb. 1993.

[9] S. D. Cheng *et al.*, ªOptimized dipole antennas on photonic bandgap crystals,º *Appl. Phys. Lett.*, vol. 67, no. 23, Dec. 1995.

[10] M. P. Kesler *et al.*, ªAntenna design with the use of photonic band-gap materials as all-dielectric planar reflectors,º *Microwave Opt. Technol. Lett.*, vol. 11, no. 4, pp. 169±174, Mar. 1996.

[11] M. M. Sigalas, R. Biswas, and K. Ho, ªTheoretical study of dipole antennas on photonic band-gap materials,º *Microwave Opt. Technol. Lett.*, vol. 13, no. 4, pp. 205±209, Nov. 1996.

[12] Y. Qian, R. Coccioli, D. Sievenpiper, V. Radisic, E. Yablonovitch, and T. Itoh, ªA microstrip patch antenna using novel photonic band-gap structures,º *Microwave J.*, vol. 42, no. 1, pp. 66±76, Jan. 1999.

[13] L. Brillouin, *Wave Propagation in Periodic Structures*, 2nd ed. New York: Dover, 1946.

[14] G. Kweon and N. M. Lawandy, ªQuantum electrodynamics in photonic crystals,º *Opt. Commun.*, vol. 118, no. 3±4, pp. 388±411, July 1995.

[15] J. R. James and A. Henderson, ªHigh-frequency behavior of microstrip open-circuit terminations,º *J. Microwaves, Opt., Acoust.*, vol. 3, pp. 205±218, 1979.

[16] R. E. Collin, *Field Theory of Guides Waves*, 2nd ed. New York: IEEE Press, 1991.

[17] R. D. Meade *et al.*, ªNature of the photonic bandgap: Some insights from a field analysis,º *J. Opt. Soc. Amer. B, Opt. Phys.*, vol. 10, no. 2, pp. 328±332, Feb. 1993.

[18] T. Baba and T. J. Matsuzaki, ªTheoretical calculation of photonic gap in semiconductor two-dimensional photonic crystals with various shapes of optical atoms,º *Appl. Phys.*, vol. 34, no. 8B, pp. 4496±4498, Aug. 1995.

[19] R. Gonzalo, ªModeling of photonic bandgap structures,º ESTEC, Eu-ropean Space Agency, AG Noordwijk, The Netherlands, Dec. 1998, ESTEC paper 2008.

[20] A. A. Maradudin and A. R. McGurn, ªOut of plane propagation of elec-tromagnetic waves in a two-dimensional periodic dielectric medium,º *J. Modern Opt.*, vol. 41, no. 2, pp. 275±284, 1994.